Polar Geosci., **17**, 156–170, 2004

Propagation and amplification of tide at the Bransfield and Gerlache Straits, northwestern Antarctic Peninsula

Walter C. Dragani[1, 2, 5*], Michael R. Drabble[3], Enrique E. D'Onofrio[1, 2, 4] and Carlos A. Mazio[1]

[1] *Departamento Oceanografía, Servicio de Hidrografía Naval and ESCM-INUN, Av. Montes de Oca 2124 (C1270ABV) Ciudad Autónoma de Buenos Aires, Argentina*
[2] *Departamento Ciencias de la Atmósfera y los Océanos, Facultad de Ciencias Exactas y Naturales, Universidad de Buenos Aires, (1428) Ciudad Universitaria, Pabellón II, 2do. piso. Ciudad Autónoma de Buenos Aires, Argentina*
[3] *Instituto Antártico Argentino. Dirección Nacional del Antártico, Cerrito 1248, (1010) Ciudad Autónoma de Buenos Aires, Argentina*
[4] *Instituto de Geodesia, Facultad de Ingeniería, Universidad de Buenos Aires, Av. Las Heras 2214, (1127) Ciudad Autónoma de Buenos Aires, Argentina*
[5] *CONICET, Consejo Nacional de Investigaciones Científicas y Técnicas*
[*] *Corresponding author. E-mail: dragani@hidro.gov.ar*

(Received October 24, 2003; Accepted July 5, 2004)

Abstract: The propagation and amplification of the tide at the Gerlache and Bransfield Straits, northwestern side of the Antarctic Peninsula, was studied by analysis of thirteen series of direct sea level measurements. Harmonic analysis was performed to obtain the amplitudes and phases of the M_2, S_2, O_1 and K_1 tidal constituents. Based on the computed harmonic constants, cotidal and corange charts of these main constituents were prepared. The M_2 cotidal lines are parallel to the coast and show predominantly southeastward propagation, except at the western side of the Trinity Peninsula, where the M_2 wave pivots to enter the Bransfield Strait from the Weddell Sea and turns southwestward. M_2 amplitudes present a southwestward decrease. S_2 cotidal lines are normal to the Antarctic Peninsula coast and show southwestward propagation. S_2 corange lines increase eastward from the Gerlache Strait to the Antarctic Strait. O_1 and K_1 cotidal lines are also normal to the Antarctic Peninsula coast. Diurnal amplitudes are alike in the study area except at the northwestern side of the Antarctic Strait where they present a maximum gradient. Amplitudes of the main tidal constituents are higher in the northwestern Weddell Sea than at the northwestern side of the peninsula. This fact explains the maximum tidal amplitudes observed at the Antarctic Strait in comparison to the Bransfield Strait.

key words: tide, measurements, cotidal and corange, northwestern Antarctic Peninsula

1. Introduction

The utility of having good knowledge about tidal dynamics and ultimately a model for tide prediction is considerable not only from the point of view of navigation but also for scientific purposes. One reason for the modern interest in tides lies in being able to compute them accurately enough so that they can be subtracted from altimetric signals,

both in the open ocean and in marginal and coastal seas (Kantha, 1995).

Tidal observations are not evenly distributed worldwide. Antarctica is one of those regions where data are scarce. Of all coastal regions in the World Ocean, the Antarctic Continent is particularly poorly served with sea level measurements, especially in the South Atlantic and South Indian Oceans (Lutjeharms *et al*., 1985). Direct measurements of sea level around Antarctica are sparse, most available measurements are from sites at shore-based laboratories. There are very few records longer than one year. Data are generally limited to the summer season because weather conditions are extremely severe during the rest of the year and coastal water often freezes. Lutjeharms *et al*. (1985) presented the geographical distribution of all tidal measurements taken along the Antarctic coastline up to 1980. There were only 75 stations at which sea level records were obtained on the Antarctic continent itself and within the adjacent coastal region. Almost fifty per cent of all measurements were situated on the western side of the Antarctic Peninsula, most of them at the Gerlache and Bransfield Straits.

The study of tidal dynamics around the whole Antarctic continent is not possible using only observations. Nevertheless, a preliminary but complete view of the tidal propagation and amplification around the Antarctica can be achieved using cotidal and corange charts obtained from global tide numerical models. The older numerical models (Schwidersky, 1979, 1981a, b, c; Cartwright and Ray, 1990) and more recently the interpretation of satellite altimeter data were used to obtain global features of the circulation and propagation of the main tidal constituents (Khanta, 1995; Matsumoto *et al*., 1995; Le Provost *et al*., 1998). The high-resolution semi-inverse global model presented by Egbert *et al*. (1994) gave a very realistic simulation of the tide at many regions around the Antarctic continent.

The main differences between observations and global ocean models arise in shallow water regions where inaccuracies in bottom depths can often cause errors as high as 100% (Kantha, 1995). Even though such global tidal models give very good results for the deep ocean, they do not have enough resolution to describe the dynamics in shelf areas close to the coast. Matsumoto *et al*. (1995) pointed out that some problems arise in some specific areas, mainly shallow water regions and step bathymentry regions. Finally, these authors pointed out the necessity of finer resolution tide models in order to improve the hydrodynamics in shallow waters.

Andersen *et al*. (1995) showed that some major differences between global models (Egbert *et al*., 1994; Sanchez and Pavlis, 1995) occur in areas close to Antarctica, where no altimetry from the Topex/Poseidon satellite exists. In the Weddell Sea, differences larger than 0.30 m are seen for semidiurnal constituents. Therefore, high-resolution local numerical models forced in their open boundaries with sea levels given by global models would have to be applied in such cases. Results given from those models would then have to be compared with direct measurements to validate the solutions. The role of ocean tides in forcing sea ice drift and periodic divergence has been recognized for at least a century (Padman and Kottmeier, 2000).

The purpose of this paper is to study the tidal propagation and amplification at the northwestern side of the Antarctic Peninsula by analysis of thirteen series of direct sea level measurements. The tidal dynamics in this region is very complex because of the

proximity to the Drake Passage where tidal waves coming from both the South Atlantic and Pacific Oceans converge. Historical data from the Instituto Antártico (IAA) and the Servicio de Hidrografía Naval (SHN) of Argentina as well as measurements gathered during the DINOCEANTAR (DINámica OCEánica ANTARtica) Project were used. The aim of the DINOCEANTAR Project (1991–1998) was to measure sea level and current in coastal waters and adjacent seas to the Antarctic Peninsula. Compared to other Antarctic areas and due to the presence of several stations of different countries, the study area was relatively well covered by tidal stations. The harmonic tidal constants (amplitudes and phases) for the four main constituents are presented. By using these harmonic constants a preliminary set of cotidal and corange charts is obtained. Finally, the propagation and amplification of the analyzed tidal constituents is discussed and compared to the scarce available literature.

2. Study area

The Gerlache and Bransfield Straits are located at the northwestern side of the Antarctic Peninsula. It is the region of the Antarctic Continent with the largest concentration of permanent scientific stations (Fig. 1). Gerlache Strait (64°30′S,

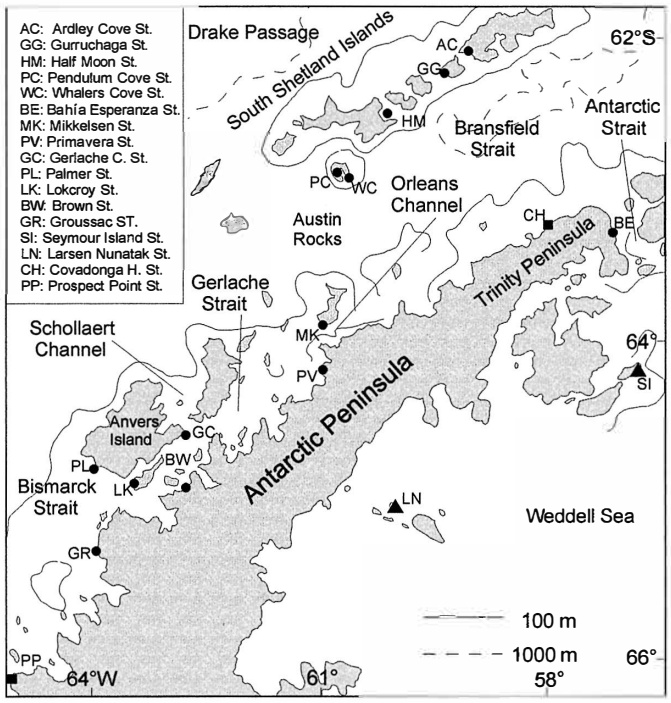

Fig. 1. Study area. Locations of the thirteen analyzed tidal stations are shown (circles). Complementary locations whose tidal constants were looked up from the Admiralty Tidal Table are included (squares). Available tidal harmonic constants corresponding to locations in the northwestern Weddell Sea are also presented (triangles). The contours of 100 and 1000 m depth are drawn.

62°20′W) is a narrow channel about 200 km long, which runs parallel to the Antarctic Peninsula in the southwest-northeast direction. Bismarck Strait and Schollaert Channel connect it to the Southeastern Pacific Ocean, and the Orleans Channel connects it to Bransfield Strait. Bransfield Strait (63°S, 59°W) is located at the northwestern side of the Antarctic Peninsula with the South Shetland Islands as its northern boundary. The Gerlache and Bransfield Straits are relatively deep, in some places greater than 1000 m. Both straits are characterized by the presence of many little islands, bays, coves and interconnected channels. Several scientific projects (*e.g.* RACER: Research on Antartic Coastal Ecosystem Rates and AMLR: Antarctic Marine Living Resources) have been conducted in the Gerlache and Bransfield Straits.

3. Background information

Tidal dynamics in Bransfield Strait is the result of superposition of two tidal waves: one coming from the South Atlantic Ocean and the other from the South Pacific Ocean.

As a first approximation, Antarctic tidal dynamics can be described using cotidal and corange charts given from modern global models (Egbert, 1994; Kantha, 1995; Le Provost *et al*., 1998). For instance, amplification of the K_1 tide around Antarctica is noteworthy, as is the M_2 tide in the Weddell Sea. Nevertheless, those models do not include the effect of sea ice, and hence the values might be overestimates.

Cotidal charts for the semi-diurnal principal lunar constituent (M_2) derived from global models show two amphidromic points, one (40°S, 110°W) in the Southeastern Pacific Ocean and the other (60°S, 0°E) in the South Atlantic Ocean northeastward of the Weddell Sea. The tidal dynamics at the northern extreme of the Antarctic Peninsula is partially given by the interaction between those two semidiurnal tidal waves. On the western side of the Antarctic Peninsula M_2 cotidal lines are almost parallel to the coast and the amplitudes increase northward. M_2 amplitudes in the Weddell Sea are higher than in the Bransfield and Gerlache Straits.

In the study area, the luni-solar diurnal constituent (K_1) cotidal is also the result of two tidal waves, one coming from the South Atlantic and the other from the South Pacific Ocean. In the southern Drake Passage, K_1 cotidal lines are almost parallel to the northwestern coast of the Antarctic Peninsula and the amplitudes, ranging from 0.2 to 0.3 m, increase toward the peninsula. The semi-diurnal principal solar constituent (S_2) presents one amphidromic point (60°S, 70°W) to the north-northwest of the Antarctic Peninsula in Drake Passage. S_2 amplitudes in the Weddell Sea are also higher than in the Bransfield and Gerlache Straits. With respect to the principal lunar diurnal constituent (O_1), cotidal lines are perpendicular to the northwestern coast of the Antarctic Peninsula and in the Bransfield and Gerlache Straits O_1 amplitudes are slightly lower than in the Weddell Sea. Cotidal and corange global charts can be obtained from Schwiderski's classical works or from any global tide model (*i.e.* Kantha, 1995; Matsumoto *et al*., 1995; Le Provost *et al*., 1998).

4. Data

The tidal data used in this work are of heterogeneous origin. Analog as well as

Table 1. List of locations where sea level was measured. Duration of each sea level record (in days) is presented. H (in m) is the amplitude, G (in degrees) is the phase lag of the tidal constituent, and e_H and e_G are their associated errors, respectively. At Brown and Bahía Esperanza Stations, amplitude errors are approximated as 0.00 m, because they are smaller than 0.005 m. Likewise, at Brown Station, M_2 and S_2 phase errors are approximated as 0°, because they are smaller than 0.5°. Locations where the phase lag of the S_2 constituent is doubtful are indicated with an asterisk. VTS: Visual Tide Staff, F: Floater, P: Pressure sensor.

Station (Code)	Lat. (S)	Lon. (W)	Type of Device	No. days	Constituents								F
					M_2		S_2		O_1		K_1		
					$H \pm e_H$	$G \pm e_G$	$H \pm e_H$	$G \pm e_G$	$H \pm e_H$	$G \pm e_G$	$H \pm e_H$	$G \pm e_G$	
Ardley Cove (AC)	62.217°	58.933°	VTS	44	.46 ± .01	276 ± 1	.25 ± .01	331 ± 1	.29 ± .01	45 ± 1	.31 ± .01	73 ± 1	0.84
Gurruchaga (GG)	62.300°	59.200°	VTS	41	.44 ± .01	279 ± 1	.23 ± .01	335 ± 1	.26 ± .01	50 ± 1	.25 ± .01	65 ± 1	0.77
Half Moon I. (HM)	62.600°	59.884°	F	38	.43 ± .01	281 ± 1	.24 ± .01	335 ± 1	.28 ± .01	49 ± 1	.28 ± .01	66 ± 1	0.84
Pendulum Cove (PC)	62.946°	60.608°	VTS	19	.44 ± .03	281 ± 4	.28 ± .03	*	.29 ± .03	55 ± 3	.26 ± .03	73 ± 3	0.76
Whalers Cove (WC)	62.983°	60.567°	VTS	12	.46 ± .03	280 ± 5	.29 ± .03	*	.29 ± .03	48 ± 4	.26 ± .03	66 ± 4	0.73
Bahía Esperanza (BE)	63.383°	56.983°	F	547	.63 ± .00	275 ± 1	.40 ± .00	312 ± 1	.40 ± .00	35 ± 1	.36 ± .00	53 ± 1	0.75
Mikkelsen (MK)	63.887°	60.733°	VTS	25	.38 ± .02	290 ± 2	.27 ± .02	7 ± 2	.33 ± .02	52 ± 2	.33 ± .02	66 ± 2	1.02
Primavera (PV)	64.150°	60.950°	VTS	44	.33 ± .01	291 ± 1	.26 ± .01	5 ± 1	.32 ± .01	59 ± 1	.31 ± .01	72 ± 1	1.07
Gerlache C (GC)	64.593°	62.890°	P	29	.29 ± .01	291 ± 1	.22 ± .01	13 ± 2	.30 ± .01	60 ± 1	.32 ± .01	78 ± 1	1.24
Palmer (PL)	64.772°	64.067°	P	30	.21 ± .01	286 ± 1	.20 ± .01	34 ± 2	.29 ± .01	69 ± 1	.32 ± .01	83 ± 1	1.49
Lokcroy (LK)	64.827°	63.492°	F	19	.23 ± .03	293 ± 3	.19 ± .03	*	.29 ± .02	68 ± 3	.29 ± .02	82 ± 3	1.36
Brown (BW)	64.900°	62.867°	F	699	.27 ± .00	291 ± 0	.20 ± .00	14 ± 0	.31 ± .00	63 ± 1	.33 ± .00	76 ± 1	1.36
Groussac (GR)	65.183°	64.167°	VTS	59	.21 ± .01	288 ± 1	.20 ± .01	32 ± 1	.29 ± .01	68 ± 1	.32 ± .01	86 ± 1	1.50

digital records exist. In the study area sea level was gathered from basic tide gauge, water level recorder with pressure sensor and visual tide staff and level. The locations where sea levels were measured are summarized in Table 1 and geographically located in Fig. 1.

From Table 1 it can be seen that in four locations sea levels were gathered by a basic tide gauge with a float and counterweight inside a vertical tube (UNESCO, 1985). At Bahía Esperanza and Brown the float had an electrical resistor in order to avoid freezing of seawater inside the tube. In this way, uninterrupted sea level series 18 months long at Esperanza and 12 months long at Brown were obtained. These analog records were digitized with one hour sampling interval. In general, standard basic tide gauges work with an accuracy of ± 0.01 m. An additional error of ± 0.01 m was assumed to be associated with the digitization procedure. Consequently, it was assumed that hourly heights obtained from analog records from a standard basic tide gauge have a total error equal to ± 0.02 m.

On the other hand, Aanderaa model TG3A water level recorder (pressure sensors) were moored in two locations during the DINOCEANTAR Project: at Gerlache C (bottom depth 90 m and instrument depth 70 m) and 400 offshore of Palmer Station (bottom depth 20 m and instrument depth 10 m). Both moorings were located near the coast in relatively sheltered places with very low currents. Consequently, in both cases, the tilt effect in the mooring line can be considered negligible. The accuracy given by the pressure sensor is approximately $\pm 0.01\%$ of the instrument depth. Sea level heights measured with pressure sensor at Gerlache C and Palmer Station had associated errors of ± 0.007 m and ± 0.001 m, respectively. These instruments were set with a sampling interval of 30 min but harmonic analyses were performed using a time interval of one hour.

In seven locations, sea level was measured with visual tide staff and level. These observations are considered to be very reliable and representative of the region because they were obtained in protected areas (coves and bays), with low wind waves and swell heights, but well connected with the open sea. Finally, the error in hourly sea level heights obtained from tide staff is not greater than ± 0.03 m.

Analyzed records significantly differ in length. There are seven sea level records of which the lengths lie between one and two months, four relatively short series lower than one month, one series of one year long and only one series longer than one year.

5. Data analysis

In this work, data were processed according to Foreman (1977) to obtain the tidal constants; associated errors were calculated using the computational methodology given by Pawlowicz *et al*. (2002). In Table 1, amplitudes H and epochs G, and their associated errors, of the principal diurnal (O_1 and K_1) and semidiurnal (M_2 and S_2) are presented, where G is the Greenwich phase (Schureman, 1988).

An important aspect of this study is related to determination of the error associated with the calculated harmonic constants. In this work sea level data series (with different duration) coming from standard tide gauge, pressure sensor and tide staff are analyzed. Consequently, each harmonic constant obtained from each data series has a

different amplitude and phase error. At Esperanza and Brown, where sea levels were measured using a standard tide gauge and the analyzed series are at least one year long, the estimated associated errors for the semidiurnal and diurnal harmonic constants are lower than 0.004 m for amplitudes and 0.5° for phases. In contrast, errors can reach up 0.03 m for amplitudes and 5° for phases at Whalers Cove, Pendulum Cove and Lokcroy, where sea level was measured with a tide staff, during lapses shorter than 20 days. The S_2 phases corresponding to the aforementioned locations were not included in Table 1 because the values obtained from the harmonic analysis are not completely reliable.

Some of the results shown in Table 1 were compared with the tidal harmonic constants corresponding to Ardley Cove (Station 2041A, 62°12′S, 58°58′W), Artigas (Station 2041B, 62°11′S, 58°52′W) and Hope Bay (Station 2043, 63°24′S, 56°59′W) in Hydrographers of the Navy (2000). A maximum difference in amplitude is detected between Hope Bay (0.57 m) and Bahía Esperanza (0.63 m) for the M_2 constituent. The other amplitudes present differences (between amplitudes obtained in this work and values published by Hydrographers of the Navy, 2000) equal or lower than 0.04 m. Phases differences are lower than 4° for all cases. Phases published by Hydrographers of the Navy (2000) are modified epochs; thus, in order to compare them with the values presented in Table 1, they must be converted to the Greenwich phase.

From Table 1 it can be seen that semidiurnal constituents have amplitudes ranging from 0.20 to 0.63 m, and the diurnal constituents from 0.25 to 0.40 m. The calculated harmonic tidal amplitudes are shown in Fig. 2. The highest amplitudes are observed at Bahía Esperanza: 0.63 m for the M_2, 0.40 m for the S_2, 0.36 m for the K_1 and 0.40 m for the O_1 constituent. The M_2 and S_2 constituents present minimum amplitudes in the southern sector of the study area (0.21 m at Groussac and 0.19 m at Lokcroy, respectively). Diurnal amplitudes are nearly uniform within the whole studied area. The O_1 and K_1 amplitudes present minimum values at Gurruchaga (0.26 m and 0.25 m, respectively).

In order to describe the tidal regime the F ratio (Defant, 1961) was calculated as:

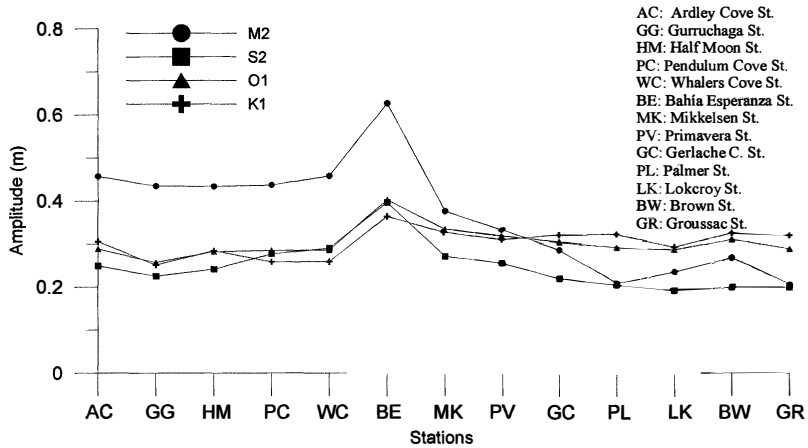

Fig. 2. Amplitudes (in m) of the computed tidal constituents for the thirteen analyzed locations.

$$F = (H_{K1}+H_{O1})/(H_{M2}+H_{S2}), \quad (1)$$

where H denotes the amplitude of each analyzed constituent (Table 1). In the Bransfield and Gerlache Straits the tide is of a mixed, mainly semidiurnal type, in agreement with the classification given by NIMA (1997). At the northwestern side of the Antarctic Peninsula the F rate increases southward because of the northward increase of the semidiurnal constituents while diurnal amplitudes are more uniform within the studied area. In contrast, in the northwestern Weddell Sea the M_2 amplitudes show southward amplification and consequently the F rate decreases southward (D'Onofrio *et al.*, 2003).

Sea level spectra corresponding to Bahía Esperanza and Brown (estimated by using

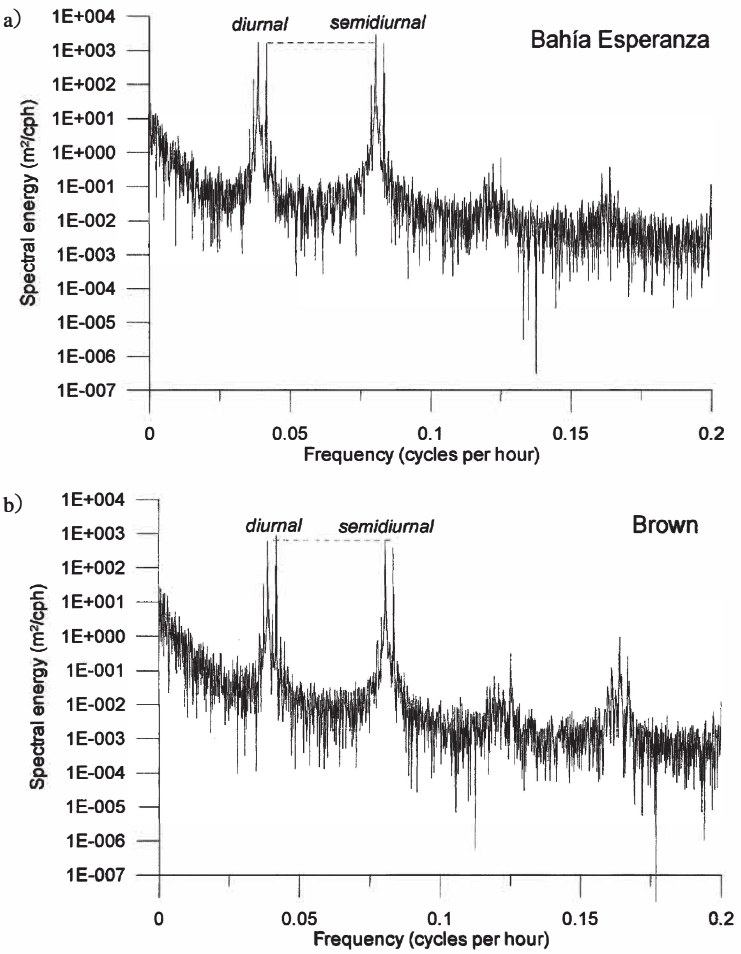

Fig. 3. Power spectra of sea levels from 18 months record of tide in Bahía Esperanza (a) and from 12 months at Brown (b). The groups of semidiurnal and diurnal spectral peaks are indicated.

the Fast Fourier Transform) are presented in Fig. 3. At Bahía Esperanza data were acquired from January 1971 to July 1972 and at Brown from January to December 1980. The group of most energetic peaks is located in the semidiurnal band in the Bahía Esperanza spectrum and in the diurnal band in the Brown spectrum. In both spectra M_2 is the most prominent constituent in the semidiurnal band. Nevertheless, in the diurnal band, the O_1 energy is greater than the K_1 energy at Bahía Esperanza; the opposite situation occurs at Brown. The combination of semidiurnal and diurnal tides produces a mixed tide. Consequently, there are intervals of several days when only diurnal tides occur and other times when the semidiurnal tide predominate.

At high frequencies, the two groups of weak spectral peaks are related to the terdiurnal and quarter diurnal tidal constituents which have associated energy three orders of magnitude lower than the diurnal and semidiurnal tides.

The cotidal and corange lines for the components M_2, S_2, O_1 and K_1 (Figs. 4 to 7) were plotted using the harmonic constants presented in Table 1. Harmonic tidal constants for Covadonga Harbor and Prospect Point (CH and PP in Fig. 1), whose values are published in the Admiralty Tide Tables (Hydrographers of the Navy, 2000), were used in this analysis when no direct measurements were available.

Cotidal and corange lines were manually drawn because computational interpolating programs did not give credible results. Cotidal and corange lines from Egbert *et al*. (1994), Kantha (1995) and Le Provost *et al*. (1998) global tide models were used as

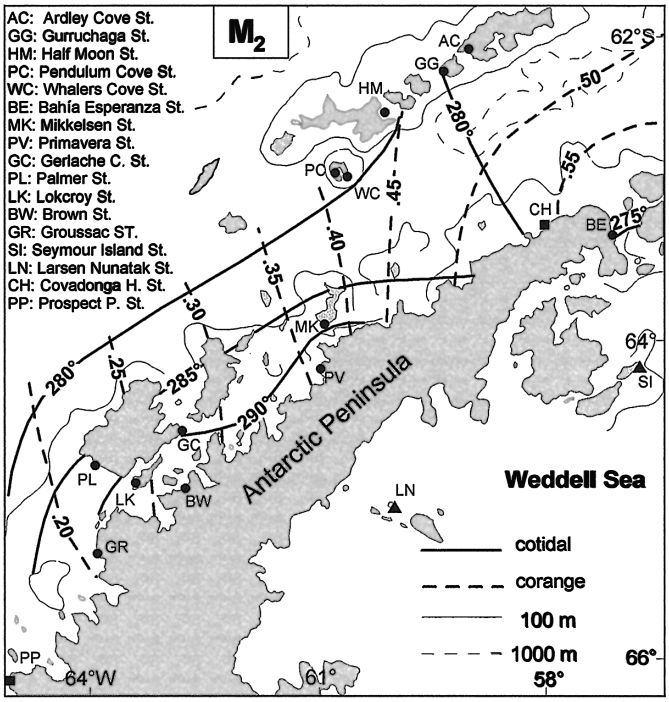

Fig. 4. M_2 cotidal (solid lines) and corange (dashed lines) constructed with harmonic constants computed from available direct measurements.

preliminary guides for constructing the tidal charts presented in this work. Based on the computed harmonic constants, cotidal and corange lines, charts of the main tidal constituents were constructed (Figs. 4 to 7). Corange lines were drawn every 0.05 m and cotidal lines, except for the M_2 constituent, every 15°. A separation of 5° was adopted for drawing the M_2 cotidal lines because this constituent presents a more reduced range for the phase (Table 1).

On the northwestern side of the Antarctic Peninsula, except around the Trinity Peninsula, the M_2 cotidals are nearly parallel to the coast (Fig. 4) and show southeastward propagation. The M_2 wave coming from the Weddell Sea enters Bransfield Strait from the northern extreme of the Antarctic Peninsula and from the Antarctic Strait. This wave turns southwestward, pivoting around the western side of the Trinity Peninsula. In this region the celerity of the M_2 wave is strongly diminished because the wave is propagated over a wide continental shelf with relatively shallow waters. The corange lines are normal to the peninsula except in northeastern Bransfield Strait where they are approximately parallel to the South Shetland Islands. Amplitudes increase from the South Shetland Islands to the Trinity Peninsula. M_2 corange lines present a progressive southwestward decrease from 0.45 m in southwestern Bransfield Strait to 0.20 m at the Gerlache Strait.

The S_2 cotidal and corange lines are presented in Fig. 5. In general, cotidal lines are normal to the Antarctic Peninsula coast and propagate southwestward. Like the

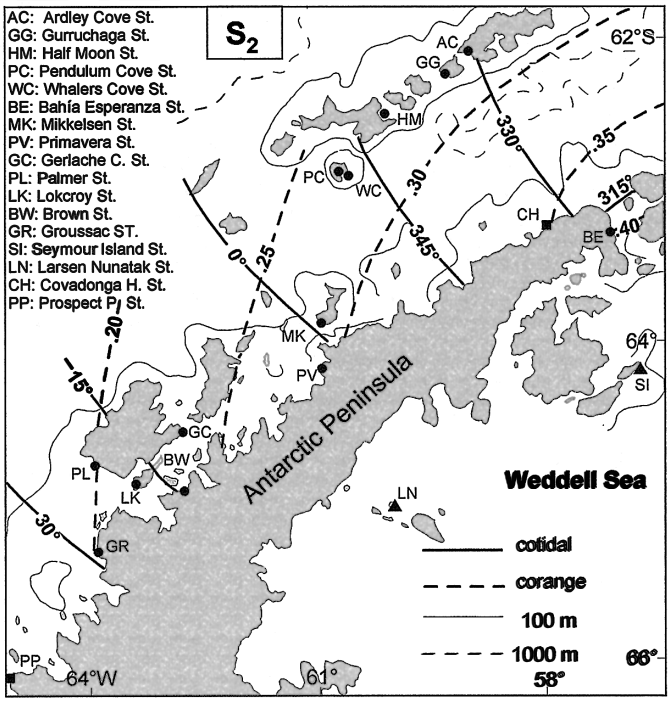

Fig. 5. Same as Fig. 4 but for S_2.

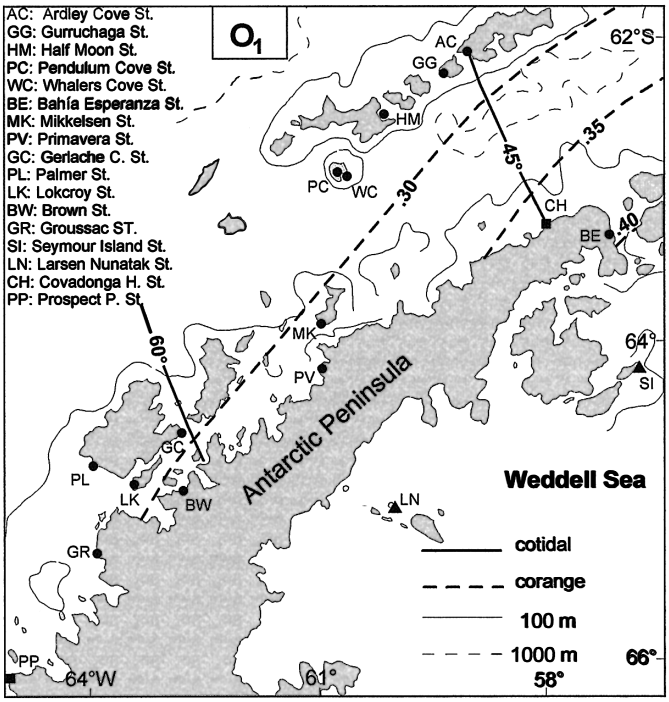

Fig. 6. Same as Fig. 4 but for O_1.

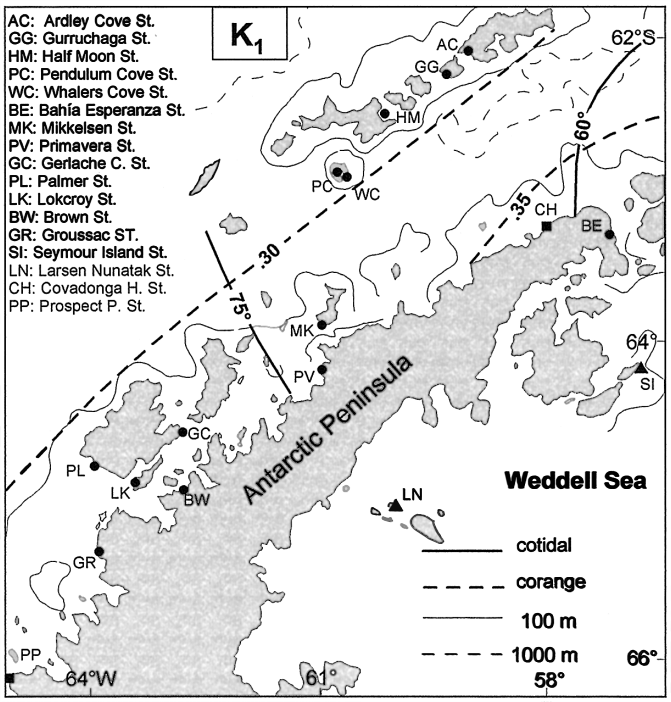

Fig. 7. Same as Fig. 4 but for K_1.

M_2 wave, the S_2 wave enters Bransfield Strait from the northern extreme of the Antarctic Peninsula and turns southwestward. On the northwestern coast of the Trinity Peninsula the phase difference between Covadonga Harbor and Bahía Esperanza is 24°, which is consistent with a relatively shallow continental shelf. In contrast, in northeastern Bransfield Strait the speed of the S_2 wave is faster, which is in agreement with a deeper region. In general, amplitudes present an eastward increase from southwestern Gerlache Strait to the Antarctic Strait. S_2 cotidal lines are normal to M_2 lines in Gerlache Strait but they are very similar to M_2 lines between the Trinity Peninsula and the South Shetland Islands.

The cotidal lines corresponding to the O_1 and K_1 tidal constituents (Figs. 6 and 7) present similar features to those of the S_2 lines. It can be seen that cotidal lines propagate southwestward in southwestern Bransfield Strait and in Gerlache Strait. Corange lines show amplitudes increasing from southwestern Gerlache Strait to the Antarctic Strait. O_1 and K_1 amplitudes are similar within the study area except on the northwestern side of the Antarctic Strait where amplitudes increase toward the Antarctic Strait and present the largest gradient.

6. Discussion

There are very few papers in the reviewed international scientific literature about sea level measurements in the Bransfield and Gerlache Straits. Consequently, comparison with previous results is rather difficult. In January 1992, an ENDECO model 1029 water level recorder was installed at the dock of Palmer Station, in Bismarck Strait. The objective of this task was to obtain tide data during the Research on Antarctic Coastal Ecosystem Rates (RACER) and Antarctic Marine Living Resources (AMLR) projects (Amos, 1993a, c). Amos (1993b) presented a discussion based on preliminary analysis of data acquired from January 1992 through May 1993. A preliminary spectral analysis showed that the principal tide is the diurnal K_1 tide with the lunar constituent O_1 nearly as prominent, in agreement with Table 1. Amos (1993b) found that the semidiurnal tide K_2 is the predominant semidiurnal constituent, closely followed by the principal lunar tide M_2. In this work, by using harmonic analysis, an amplitude of 0.05 m for the K_2 tidal constituent was obtained at Palmer, that is to say, only one quarter of the computed M_2 tidal amplitude. Although Amos' sea level series (17 months long) is longer than the record analyzed in this work (one month long) the main difference found at the semidiurnal band could be explained because sea level data have been processed differently. Whereas Amos applied spectral analysis for processing sea level data, in this work the data were processed using harmonic analysis, which is more convenient for computing tidal harmonic constants.

Klinck (1995) compared the simulated tidal structure from the Oregon State University (OSU) Model (Egbert *et al*., 1994) with that measured at Palmer Station. Comparison between simulated and observed tides showed good general agreement. The larger differences between observed and modeled values had a range of $+0.4$ to -0.5 m, probably caused by wind and atmospheric pressure effects. The periods of semidiurnal and diurnal tides agreed, although the simulated semidiurnal amplitude was larger than that measured. In general, results obtained from the OSU Model agree well

with sea level measured in relatively open areas, like Palmer in Bismarck Strait, which is connected with the Bellingshausen Sea. Nevertheless, global models do not give satisfactory agreement when their results are compared with direct measurements in shallow water or very close to the coast. For instance, due the relatively low resolution of tide global models, sea levels at sites located in Gerlache Strait or the Antarctic Strait can not be accurately reproduced.

The higher amplitude close to the Antarctic Strait is an important feature that can be seen in Figs. 4 to 7. It is a direct consequence of the free connection between the Weddell Sea and the northwestern side of the peninsula. In general, tidal amplitudes are higher in the western Weddell Sea than in the Bransfield and Gerlache Straits. The amplification and propagation of the tide in the northwestern Weddell Sea was studied by analysis of direct measurements by Foldvik *et al*. (1990), Robertson *et al*. (1998), Speroni *et al*. (2000) and D'Onofrio *et al*. (2003). Sea levels were measured at the northeastern coast of Seymour (Marambio) Island (SI in Fig. 1) and at Larsen nunatak (LN in Fig. 1), at the edge of the Larsen ice-shelf, in the northeastern side of the Antarctic Peninsula. By means of harmonic analysis the amplitudes and phases of the most energetic tidal constituents were obtained. The tidal regime was described by means of F and a mixed, mainly semidiurnal type, was also obtained. Significant southward amplification was observed in the amplitudes of semidiurnal constituents, and less evident amplification in diurnal ones. Slightly southward diminution in the F rate, from 0.75 (Bahía Esperanza) to 0.60 (Larsen nunatak, at the edge of the Larsen ice-shelf), was found. Considering the results obtained in this work and those given by D'Onofrio *et al*. (2003) it can be concluded that semidiurnal amplitudes (M_2 and S_2) are reduced progressively around the northern extreme of the Antarctic Peninsula, from Nunatak Larsen, at the Weddell Sea (0.83 m and 0.55 m, respectively) to Groussac, and southward to Bismarck Strait (0.21 m and 0.20 m, respectively).

Diurnal amplitudes present similar features to semidiurnal amplitudes around the tip of the Antarctic Peninsula but diurnal amplitudes are significantly lower than semidiurnal ones in the Weddell Sea. Diurnal amplitudes (O_1 and K_1) are also attenuated from Nunatak Larsen (0.40 m and 0.43 m, respectively) to southern Gerlache Strait (0.29 m and 0.32 m, respectively).

Tidal dynamics at Gerlache Strait were analyzed; the small phase difference between northern and southern Gerlache Strait (phase differences between Brown and Primavera are 0° for the M_2 constituent, 9° for the S_2 and 4° for the O_1 and the K_1) suggest that the water level rises and falls almost uniformly throughout Gerlache Strait.

Even though the tidal dynamics on the northwestern side of the Antarctic Peninsula have been analyzed and discussed, direct measurements, especially at Bransfield Strait, are scarce. In this region, sea level measurements were taken at locations on the northwestern coast of the Trinity Peninsula and in the South Shetland Islands. There are not observations taken in the middle of the strait, in the open sea, or between the peninsula and the South Shetland Islands. Although much effort has been put in measuring sea level in Bransfield Strait, the results have been rather limited. Because of this, within this broad strait (100 km wide) the cotidal and corange lines shown in this paper could present some uncertainty.

The set of cotidal and corange charts presented in this work should give us a fairly

good understanding of the tidal dynamics on the northwestern side of the Antarctic Peninsula. The main uncertainties are located in Bransfield Strait, where sea level measurements are necessary not only to obtain a realistic view of tidal propagation within the study region but also to better understand the tidal dynamics at the northeastern tip of the Antarctic Peninsula between the Weddell Sea and Bransfield Strait.

References

Amos, A.F. (1993a): Research on Antarctic coastal ecosystem rates (RACER) program. Antarct. J. U. S., **28** (5), 157–158.

Amos, A.F. (1993b): RACER. The tides at Palmer Station. Antarct. J. U. S., **28** (5), 162–164

Amos, A.F. (1993c): AMLR program: Interannual variability in the Elephant Island surface waters in the austral summer. Antarct. J. U. S., **28** (5), 201–204.

Andersen, O.B., Woodworth, P.L. and Flather, R.A. (1995): Intercomparison of recent ocean tide models. J. Geophys. Res., **100**, 25261–25282.

Cartwright, D.E. and Ray, R.D. (1990): Oceanic tides from Geosat Altimetry. J. Geophys. Res., **96**, 16897–16912.

Defant, A. (1961): Physical Oceanography, Vol. II. Oxford, Pergamon Press, 598 p.

D'Onofrio, E.E., Dragani, W.C., Speroni, J.O. and Fiore, M.E. (2003): Propagation and amplification of tide at the northwestern coast of the Antarctic Peninsula: an observational study. Polar Geosci., **16**, 53–60.

Egbert, G.D., Bennett, A.F. and Foreman, M.G.G. (1994): TOPEX/POSEIDON tides estimated using a global inverse model. J. Geophys. Res., **99**, 24821–24852.

Foldvik, A., Middleton, J.H. and Foster, T.D. (1990): The tides of the southern Weddell Sea. Deep-Sea Res., Part A, **37**, 1345–1362.

Foreman, M.G.G. (1977): Manual for tidal heights analysis and prediction. Pac. Mar. Sci. Rep., **77–10**, 97 p.

Hydrographers of the Navy (2000): Admiralty Tide Tables, Europe (excluding United Kingdom and Ireland), Mediterranean Sea and Atlantic Ocean, Vol. 2, NP 202–01–2001.

Kantha, L.H. (1995): Barotropic tides in the global oceans from a nonlinear tidal model assimilating altimetric tides. 1. Model description and results. J. Geophys. Res., **100**, 25283–25308.

Klinck, J.M. (1995): Palmer LTER: Comparison between a global tide model and observed tides at Palmer Station. Antarct. J. U. S., **30** (5), 263–264.

Le Provost, C., Lyard, F., Molines, J.M., Genco, M.L. and Rabilloud, F. (1998): A hydrodynamic ocean tide model improved by assimilating a satellite altimeter-derived data set. J. Geophys. Res., **103**, 5513–5529.

Lutjeharms, J.R.E., Stavropoulos, C.C. and Koltermann, K.P. (1985): Tidal measurements along the Antarctic Coastline. Oceanology of the Antarctic Continental Shelf. Washington, D.C., Am. Geophys. Union, 273–289 (Antarct. Res. Ser., **43**).

Matsumoto, K., Ooe, M., Sato, T. and Segawa, J. (1995): Ocean tide model obtained from Topex/Poseidon altimetry data. J. Geophys. Res., **100**, 25319–25330.

NIMA (1997): Sailing Directions (Planning Guide and Enroute), Antarctica. National Imagery and Mapping Agency, 3rd. ed., Bethedsa, 177 p.

Padman, L. and Kottmeier, C. (2000): High-frequency ice motion and divergence in the Weddell Sea. J. Geophys. Res., **105**, 3379–3400.

Pawlowicz, R., Beardsley, B. and Lentz, S. (2002): Classical Tidal Harmonic Analysis Including Error Estimates in MATLAB using T_TIDE. Comput. Geosci., **28**, 929–937.

Robertson, R.A., Padman, A.L. and Egbert, G.D. (1998): Tides in the Weddell Sea. Ocean, Ice and Atmosphere: Interactions at the Antarctic Continental Margin, ed. by S.S. Jacobs and R.F. Weiss. Washington, D.C., Am. Geophys. Union, 341–369 (Antarct. Res. Ser., **75**).

Sanchez, B. and Pavlis, N.K. (1995): Estimation of the main tidal constituents from Topex/Poseidon

altimetry using a Proudman function expansion. J. Geophys. Res., **100**, 25011–25022.

Schureman, P. (1988): Manual of harmonic analysis and prediction of tides. Washington, U.S. Government Printing Office, Special Publ. No. 98, 317 p.

Schwiderski, E.W. (1979): Global ocean tides, Part II: the semidiurnal principal lunar tide (M_2), atlas of tidal charts and maps. Dahlgen: Naval Surface Weapons Center, NSWC TR 79–414.

Schwiderski, E.W. (1981a): Global ocean tides, Part III: the semidiurnal principal solar tide (S_2), atlas of tidal charts and maps. Dahlgen: Naval Surface Weapons Center, NSWC TR 81–122.

Schwiderski, E.W. (1981b): Global ocean tides, Part IV: the diurnal luni-solar declination tide (K_1), atlas of tidal charts and maps. Dahlgen: Naval Surface Weapons Center, NSWC TR 81–142.

Schwiderski, E.W. (1981c): Global ocean tides, Part V: the diurnal principal lunar tide (O_1), atlas of tidal charts and maps. Dahlgen: Naval Surface Weapons Center, NSWC TR 79–144.

Speroni, J.O., Dragani, W.C., D'Onofrio, E.E., Drabble, M.R. and Mazio, C.A. (2000): Estudio de la marea en el borde de la barrera Larsen, Mar de Weddell noroccidental. Geoacta, **25**, 1–11.

UNESCO (1985): Manual on sea level measurement and interpretation. Intergovernmental Oceanographic Commission, 83 p.